MethodsX 8 (2021) 101539

Contents lists available at ScienceDirect

MethodsX

journal homepage: www.elsevier.com/locate/mex

Method Article

Method of developing Thermo–Kinetic diagrams: The Cu–H_2O–acetate and the Cu-H_2O systems

Kashif Mairaj Deen*, Edouard Asselin

Department of Materials Engineering, The University of British Columbia, Vancouver, BC V6T 1Z4, Canada

A B S T R A C T

A method to develop thermo-kinetic (TK) diagrams for the Cu–H_2O–acetate and Cu–H_2O systems is described. Conventional E_h-pH diagrams, also known as Pourbaix diagrams, are developed based on the thermodynamic stability of component species, typically in aqueous media. TK diagrams are an improvement on E_h-pH diagrams as they also describe the kinetics of electrochemical processes. These diagrams are developed by using data from linear scan voltammetry of Cu rotating disk electrodes exposed to aqueous media of different pH. By applying the same procedure, the TK diagrams can be developed for other metals or mineral systems exposed to aqueous media containing ligands. To ensure reproducibility and reconstruction of the TK diagrams for other metal/mineral/electrolyte systems, some important experimental considerations are highlighted in this study. These TK diagrams are useful to evaluate the corrosion of metals, the leaching performance of minerals and to predict the suitable conditions for metal recycling processes.

Briefly, this article explains:

- Important experimental considerations that could affect the kinetics of electrochemical processes.
- A method to construct TK diagrams with examples of the Cu–H_2O–acetate and Cu–H_2O systems.
- With overlaid E_h-pH diagrams, TK diagrams explain both the thermodynamic stability of component species and the kinetics of the electrochemical processes.

A R T I C L E I N F O

Method name: A method to develop thermo-kinetic (TK) diagrams
Keywords: Pourbaix diagrams, Copper leaching, Corrosion, Hydrometallurgy, Electrochemical, Linear Scan Voltammetry
Article history: Received 18 June 2021; Accepted 3 October 2021; Available online 6 October 2021

DOI of original article: 10.1016/j.jelechem.2021.115467

* Corresponding author.
E-mail address: deen@mail.ubc.ca (K.M. Deen).

https://doi.org/10.1016/j.mex.2021.101539

Specification table

Subject Area	Applied Electrochemistry
Specific Subject Area	Aqueous processing of metals
Method Name	A method to develop thermo-kinetic (TK) diagrams
Original Method Name and Reference	Establishment of Eh-pH diagrams (Pourbaix Diagrams) ***Reference***: *Marcel Pourbaix, Atlas of Electrochemical Equilibria in Aqueous Solutions, 1974, NACE, Houston, TX*
Resource Availability	N.A.

Background

The thermodynamic stability of chemical and electrochemical species in aqueous media can be evaluated from the conventional E_h-pH, also known as Pourbaix, diagrams. The stability of these species and the conversion of one species to another under equilibrium conditions can be described thermodynamically and displayed by regions separated by lines on the E_h-pH plane [1]. These diagrams are important to predict the suitable process conditions (i.e. temperature, pressure, potential, pH, presence of ligands and complexation) for metal extraction and recovery, mitigating or controlling metal corrosion and estimating the solubility and precipitation of ionic species formed by various processes, such as the weathering of natural minerals. However, the construction of the E_h-pH diagrams depends on the availability of thermodynamic data and on rigorous calculations that only correspond to equilibrium conditions. However, the availability and reliability of such thermodynamic data, for many species, such as complexes, remains a challenge. In addition, these diagrams express equilibrium conditions and are incapable of describing the kinetic details of either chemical or electrochemical processes. For instance, practically, metal corrosion and mineral leaching processes take place far away from equilibrium and the formation of intermediate or final products may not be accurately predicted using existing E_h-pH diagrams.

For these reasons, the concept of the TK diagram is introduced [2]. Roy et al. [3] developed the TK diagram for the Fe-NH_3-CO_3-H_2O system by measuring the potentiodynamic polarization scans of Fe in solutions having different pH. The polarization curves were obtained in stationary solutions at 25 °C and, based on the current response, the corrosion (E_{corr}) and peak (E_{peak}) potentials were measured at each pH ranging from 4 to 14. The potential values were overlaid on the E_h–pH diagram to describe the actual potential range of active Fe dissolution under applied conditions. However, from these TK diagrams, it was difficult to directly decipher the kinetic information. Similarly, an experimental Pourbaix diagram of Fe in 0.01 M Cl^- solution was developed based on cyclic polarization test results [4]. The E_{corr}, E_{peak} and protection potential values were determined from polarization curves obtained in different pH solutions. These values were plotted on the E_h-pH scale to differentiate between general corrosion, pitting, perfect and imperfect passivation regions. It is important to mention here that many metals in different electrolytes (i.e. Fe, Zn, and Cu in acidic solutions) do not exhibit active-passive dissolution behavior and determination of E_{peak} and/or protection potential is almost impossible. To address these issues an improved method for generating TK diagrams is introduced, the construction of which uses experimental current-potential data obtained under optimized conditions. For instance, with the support of E_h-pH diagrams, different regimes in the TK diagrams can be differentiated by the magnitude of the current density measured at each potential and pH. These current values can be used to estimate the rate of electrochemical processes under various applied conditions. In addition, these diagrams can be developed by using experimental electrochemical data for any metal, alloy, or mineral exposed to any aqueous or ligand-containing media. However, it is important to optimize the experimental conditions before measuring the current response during electrochemical testing. It is proposed that either alone, or in combination with E_h-pH diagrams, these TK diagrams could be beneficial for informing process decisions such as hydrometallurgical metal extraction, metal recycling, corrosion/dissolution behavior and in estimating the extent of parasitic reactions (e.g. H_2 or O_2 evolution). As examples, the TK diagrams of the Cu-H_2O-acetate and Cu-H_2O systems are constructed experimentally under optimized conditions. To construct reproducible TK diagrams a detailed methodology is presented and some important considerations are highlighted below.

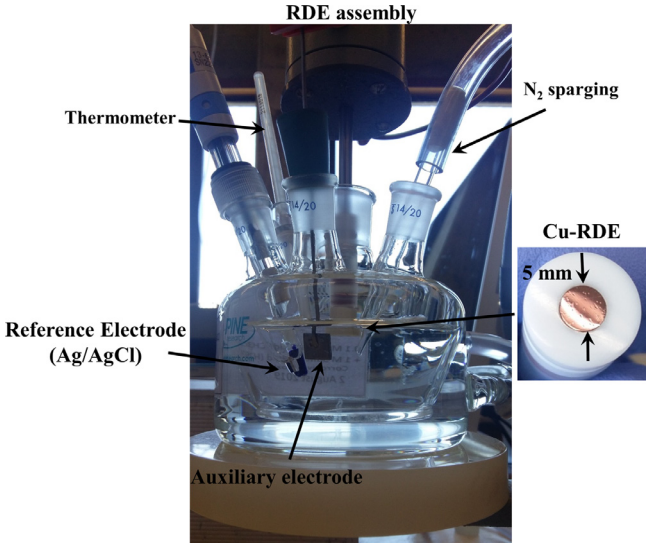

Fig. 1. A water-jacketed three-electrode cell assembly used to measure the electrochemical response of the Cu-RDE (Note: Pt square disk of 2.2 cm^2 surface area was used as the auxiliary electrode, Single junction saturated KCl Ag/AgCl (Fisherbrand™ accumet™, 13-620-216) was used as reference electrode).

Method details

Considerations in sample and solution preparation

A Puratronic® pure copper (Cu 99.999%) rod (5 mm in diameter) purchased from VWR™, USA, was used to prepare the disk samples of 4 mm in thickness. The disk samples were cut using electrical discharge wire-cutting machining to minimize the heating during the cutting process. Overheating of the metallic samples should be avoided during the cutting process because it may affect microstructural features and may alter the electrochemical response. For heat-sensitive materials, a post-stress relieving heat treatment procedure could be adopted. Due to the high thermal conductivity of pure Cu, no significant effect on the microstructure was observed due to the cutting process. It is important to emphasize the sample preparation procedure to avoid variation in the current response. Cu disks were ground by using successive silicon carbide paper of increasing grit numbers from P1000 to P1500 to P2000. Finally, the Cu-disk samples were sequentially polished on a long napped rayon cloth impregnated with Al_2O_3 particles having the size of 5 and then 1 µm to produce a mirror-like surface. The polished disks of 0.196 cm^2 exposed surface area were inserted in PTFE tips and attached to the rotating disk assembly (E4TQ ChangeDisk, PINE Research): this assembly is referred to as a Cu rotating disk electrode (Cu-RDE) in the following discussion. The polished samples were washed ultrasonically with deionized (DI) water for 10 min before immersion in the electrolytes of known pH stabilized at a constant temperature of 25 °C in a thermostatic water-jacketed cell.

Electrolytes of different pH ranging from 0.5 to 13 were prepared by adding a calculated amount of chemical reagents of industrial-grade purity. A fresh solution of particular pH was prepared right before each experiment and pH was stabilized at a constant temperature of 25 ± 1.0 °C, by the temperature control method described above. Nitrogen gas of 99.95 % purity was bubbled through the solution for 30 min to deaerate the electrolytes – no bubbling occurred after this initial purging. All the electrochemical tests were conducted in a water-jacketed three-electrode cell assembly (AKCELL3, PINE Research) as shown in Fig. 1. In each experiment, 100 ml of the electrolyte was added to the cell. The water jacket of the cell was connected to a thermostated circulating water bath that controlled

the temperature of the electrolytes within the cell. The polished Cu-RDE, platinum (2.2 cm^2) auxiliary and Ag/AgCl (sat. KCl) reference (0.199 V vs. standard hydrogen electrode; SHE) electrodes were directly installed in the cell without a Luggin capillary. The reference electrode was calibrated after every 20 h of use. Before each test, the cell assembly was kept idle for an hour to achieve thermal equilibrium between cell components. All further potential values are reported vs. the SHE scale and unless stated otherwise.

The key considerations in data collection and development of TK-diagrams

In our previously published work, the TK-diagram of the $Fe-NH_3-CO_3-H_2O$ system was developed through electrochemical measurements [3]. As a function of applied potential, pure Fe presents active/passive behavior in ammoniacal solution under deaerated conditions. The corrosion potential (E_{corr}) and peak potential (E_{peak}) values were used to construct the TK diagrams. Where E_{corr} is the equilibrium potential that is established between metal and electrolyte and E_{peak} represents the thermo-kinetic equilibrium potential of the metal at which it transformed from the active to the passive state. This method implied that such diagrams can only be constructed for metals that present active/passive electrochemical responses when exposed to particular electrolytes. However, the very active metals such as Mg and Zn in aqueous media may not show passive behavior and the construction of such TK-diagrams becomes difficult for these systems when using only the potential data. Esmiazadeh et al. [5] explained that the potential range between E_{corr} and E_{peak} (primary passive potential) represents the region within which metal dissolves and metal ions are thermodynamically more stable. This region is typically designated as the corrosion region in the E_h-pH diagram. The alternative approach, and the one that is used here, is to use potential vs. current data obtained from potentiodynamic polarization scans and plotted as a function of pH.

However, there are many challenges in obtaining reliable and reproducible polarization data. For instance, electrode surface conditions, selection of potential sweep rate, the effect of complexing agents, variation in temperature and pH of the electrolytes, control of hydrodynamic conditions and continuous supply of ionic species at the electrode/electrolyte interface are important factors and must be considered to develop the TK-diagrams on the E_h-pH-*i* scales. The potential sweep rate (dV/dt) should be selected low enough to ensure that the current response (I_t) only corresponds to the charge transfer processes (faradaic current; I_f) having minimum current contribution associated with the non-faradaic processes i.e. double layer charging (c) as given in equation E1 according to ASTM G102-89 (2015).

$$I_t = I_f + c\left(\frac{dV}{dt}\right) \tag{1}$$

To avoid the overestimation of the current response, it is important to conduct the impedance analysis of the electrode/electrolyte system as proposed by Mansfeld and Kendig [6]. As a general criterion, it is stated that for passive metals, which present high polarization resistance ($\geq$ 10 kΩ-cm^2) or low current density $\sim$ 1 μA/cm^2, the potential sweep rate must be selected as $<$ 1 mV/s. For this reason, in this study, a potential sweep rate of 0.1667 mV/s was selected for the Linear Scan Voltammetry (LSV) measurements.

Similarly, to ensure the continuous supply of ionic species at the electrode/electrolyte interface or, in other words, to avoid diffusion limitations, a rotating disk electrode (RDE) assembly was used to measure the current (i_k) of Cu exposed to electrolytes of different pH. To minimize the current contribution associated with mass transport an optimized rotation rate was selected. The well-defined hydrodynamic conditions and mass transport characteristics of the RDE system are expressed by the Koutecky-Levich equation E2 [7].

$$\frac{1}{i} = \frac{1}{i_k} + \frac{1}{ABC_o\omega^{0.5}} \tag{2}$$

The second term in this equation is related to the diffusion-limited current and can be neglected if a sufficiently large rotation rate is selected. In this relation, A is the surface area of the (Cu) disk exposed to the electrolyte whereas $B = 0.62nFD^{2/3}\upsilon^{-1/6}$. The terms C_o, ω, n, F, D, and υ represent the

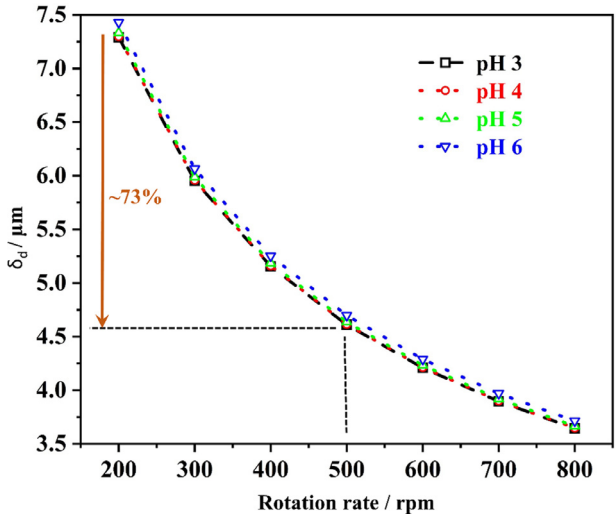

Fig. 2. Effect of Cu-RDE rotation rate on the diffusion layer thickness as a function of solution pH.

concentration of the ionic species (moles/litre), angular velocity (rad/s), number of electrons, Faraday's constant (96485 C/mol), diffusion coefficient (cm^2/s) and kinematic viscosity (cm^2/s), respectively. The thickness of the diffusion layer (δ_d) depends on the diffusion coefficient of the ionic species, the kinematic viscosity and the rotation rate, as given in equation E3.

$$\delta_d = 1.61 D^{1/3} \nu^{1/6} \omega^{-1/2} \tag{3}$$

The density, ionic conductivity, and kinematic viscosity of each acetic acid/acetate buffer solution (pH 3–6) were experimentally measured and D was assumed to be 10^{-5} cm^2/s (for dilute solutions) based on the rigorous experimentation and calculations of diffusion coefficients of ionic species in acetic acid/sodium acetate/H_2O buffer solutions by Derek et al. [8] The detailed results and calculations to determine δ_d are given in the *supplementary data set sheet*. It is important to select an appropriate rotation rate (or angular velocity) to reduce the mass transport effects on the kinetic response of the Cu-RDE during LSV scanning. The rotation rate has a significant influence on the hydrodynamic and diffusion layer thickness that could ultimately affect the kinetic response of the Cu-RDE. The δ_d decreases with an increase in rotation rate and was found to be independent of the solution pH. An approximately 73% decrease in δ_d was observed at 500 rpm (52.3 1/s) as shown in Fig. 2. A 500 rpm rotation rate was selected as further increases in RDE rpm would not have significantly changed δ_d. However, other metal/electrolyte systems having variable flow characteristics and physical properties i.e. density and viscosity of the solution could affect the hydrodynamic and diffusion layer thickness and must be taken into account for the selection of appropriate RDE rotation rate and can be ascertained by following the same procedure. In addition, the current response could vary as a function of Cu-RDE rotation rate due to the presence of complexing species in the electrolyte and the formation of intermediate species at the surface of the electrode could also affect the current response as evident in Fig. 3a. At pH 6, in acetate buffer solution, the current response of the Cu-RDE increased with an increase in its rotation rate up to 500 rpm possibly related to the reduction in δ_d. However, further increase in rotation rate to 700 rpm resulted in the decrease of current as exhibited by peaks 1, 2 and 3 in Fig. 3a. Based on the E_h–pH diagram, the slight shift in peak potentials to higher values, and decrease in current response at rotation rate $>$ 500 rpm, is likely due to the formation of adsorbed species (i.e. $Cu(CH_3COO)_2$) on the surface of the Cu-RDE. However, further in-situ surface characterization (perhaps via a ring-disk electrode assembly) is required to confirm the formation of intermediate species on the Cu-RDE surface. At pH 9 the limiting current response of the Cu-RDE remained independent of the rotation rate and corresponded to the formation of a surface

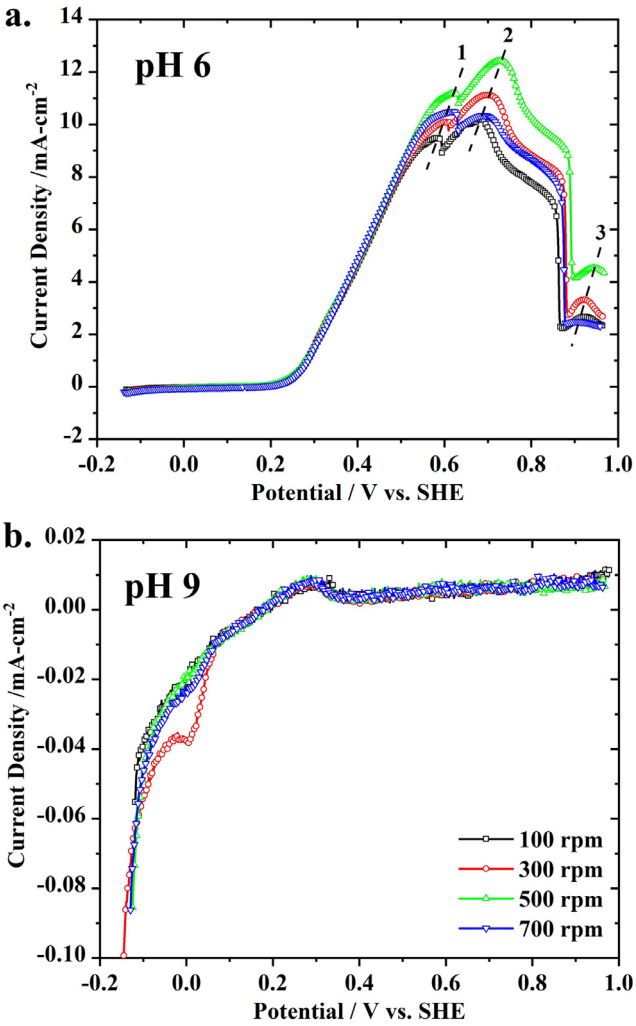

Fig. 3. Effect rotation rate on the current response of Cu-RDE in electrolytes of (a) pH 6 and (b) pH 9.

passive film (Fig. 3b). The decrease in δ_d at rotation rates above 500 rpm would reduce the effect of mass transport limitations at the electrode/electrolyte interface, however, as explained above, the current response was mostly associated with the kinetic behavior of the Cu-RDE and complexation of the dissolved species. The adsorption of intermediate species that do not escape the surface at high rpm (as a function of pH) could significantly impact the current response as evident in Fig. 3a.

It is cumbersome to measure the current response at each potential and pH using potentiostatic (PS) methods (especially within a large range such as the –0.5 to 1.0 V vs. OCP range used here). However, both LSV and PS tests were conducted to compare the electrochemical response and validate the use of LSV curves for the bulk of the measurements that support the TK diagrams. An initial delay of 2 h was imposed to measure the OCP of the polished Cu-RDE to verify the establishment of steady-state conditions (~0.1 mV/min) within the cell. As explained in the main text, the PS and LSV methods resulted in similar currents with a maximum difference of ±10%. This further justified the selection of the experimental parameters (i.e. slow potential sweep rate of 0.1667 mV/s and rotation rate of

Table 1
Calculated mean current and uncertainty values for Cu-H_2O-Acetate system. The total number of experimental values (n) = 4. (see Supplementary dataset excel sheet ("Uncertainty") for further information).

pH	200 mV		400 mV		600 mV	
	μ (A)	±U (A)	μ (A)	±U (A)	μ (A)	±U (A)
3	7.4E-05	3.2E-06	1.7E-04	6.7E-06	2.7E-04	1.0E-05
5	5.9E-04	4.5E-06	1.3E-03	5.0E-05	1.1E-03	6.5E-05
7	5.7E-06	5.4E-07	6.1E-06	4.5E-07	6.1E-06	5.0E-07
9	3.5E-07	7.0E-09	6.8E-07	7.1E-09	8.2E-07	1.1E-08
11	2.5E-06	3.9E-07	1.1E-06	1.1E-07	1.4E-06	1.1E-07
13	5.2E-06	7.7E-07	5.3E-06	1.9E-07	5.5E-06	1.9E-07

500 rpm etc.) that were used for the construction of the TK diagrams. Also, the LSV tests of the Cu-RDE samples were repeated four times at all pH under the same conditions to ensure reproducibility and to estimate the uncertainty in the current response. At each pH, from 4 different LSV curves, the current values obtained at different potentials (i.e. 200, 400 and 600 mV vs. Ag/AgCl) were used to calculate the uncertainty in the test results. The uncertainty (U) or ± error values (in 'A' units) are calculated from the mean current values (μ) at different pH by using equation E4 [9] and are given in Table 1.

$$U = \sqrt{\frac{\sum (x_i - \mu)^2}{n(n-1)}} \tag{4}$$

Where 'x_i' is the current value in amperes (A) and 'n' is the total number of current values at each pH and a given potential or number of LSV tests conducted to verify the reproducibility in the results. The detailed calculation procedure is added in the *Supplementary dataset sheet (designated as "Uncertainty")*. Compared to μ, very small U values indicate the validity of the LSV test data used to construct the TK diagram for the Cu-H_2O system. The same methodology may be applied to other systems to validate the reproducibility of the LSV data and to predict the reliability of TK diagrams in terms of ± error or uncertainty.

The TK diagrams of the Cu-H_2O-acetate and Cu-H_2O systems were developed using the procedure described above and compared with the calculated E_h-pH diagrams [10]. The LSV data was exported and processed in Origin® 2018 Graphing and Analysis software. The stepwise procedure to draw the contour plots in Origin® graphing software is presented in Fig. 4. The E_h-pH-i contour plots were drawn and overlayed with calculated E_h-pH diagrams of the Cu-H_2O-acetate and Cu-H_2O systems for presenting both the kinetic and thermodynamic information. Further detail and stepwise plotting procedure can be obtained at https://www.originlab.com/doc/Tutorials/Contour-Color-Map.

Briefly, the first step is to export the LSV and thermodynamic (Eh-pH) data to the Origin software followed by plotting the contour maps as presented in step-2. The final TK diagram of the Cu-H_2O-acetate systems is shown in step-3. To reproduce these diagrams, the complete data of LSV test results and thermodynamic calculations are given in the *supplementary information*.

The example construction of a TK diagram for the Cu-H_2O system is presented in Fig. 5. The pH of the solutions was adjusted by adding either H_2SO_4 or NaOH in DI water at 25 °C without buffering agents. The LSV scans obtained at each pH (1–7) were plotted on the semi-logarithmic scale to display the current response (Fig. 5a shows only examples at pH 2, 4 and 6). For instance, three selected points (a, b and c) on each polarization curve (Fig. 5a) are indicated at each pH (2, 4, 6) on the TK diagram shown in Fig. 5b. It is important to note that to develop the actual TK diagram, the polarization scans were obtained from –0.3 to 1.2 V vs. SHE at a scan rate of 0.1667 mV/s containing ~1000 data points: each of these points was used in the contour map. In other words, at any specific pH, the current density value at each potential corresponds to the specific region on the contour map (on the Eh-pH-i scale). The magnitude of current density measured at each pH and potential is represented in the TK diagram by different color regimes. In combination with the E_h-pH diagram of the Cu-H_2O system, the interactive display of the current response in the TK diagram is beneficial in estimating the overall rate of the electrochemical processes. The same procedure can be adopted for

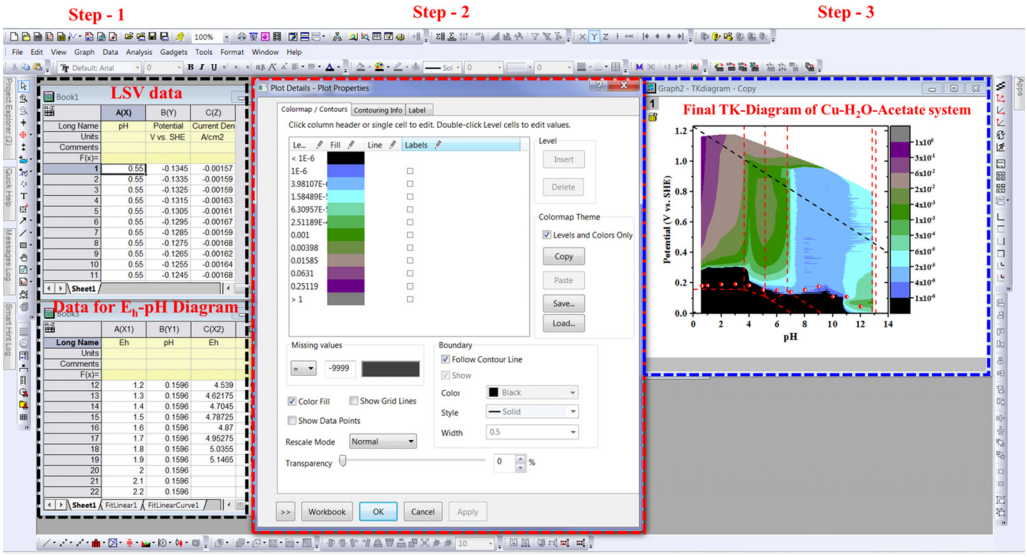

Fig. 4. Stepwise procedure of plotting the contour plots (TK-diagrams) on Origin® 2018.

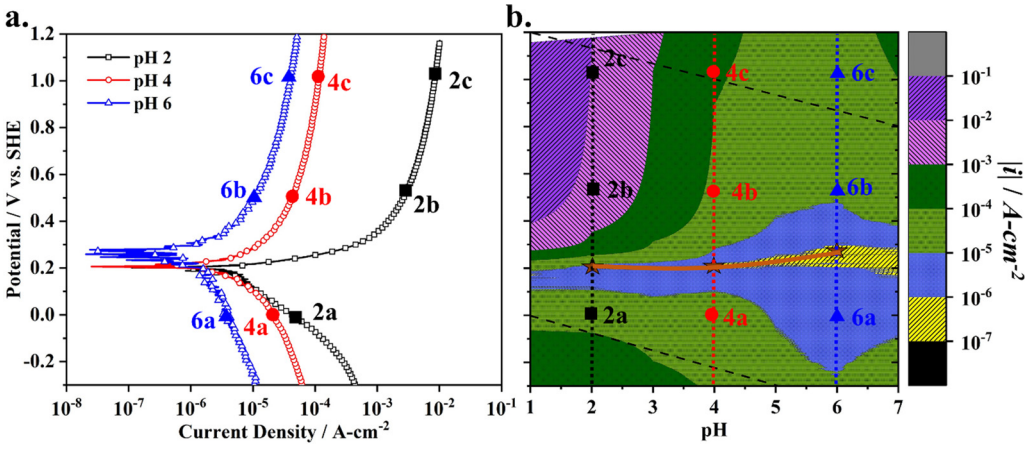

Fig. 5. Example construction of the TK diagram for the Cu-H_2O system (a) LSV test results obtained at different pH (potential sweep rate 0.1667 mV/s, 500 rpm) (b) final TK diagram for the Cu-H_2O system indicating the current response on E_h-pH scale at 25 °C. (Note: the star symbols, and the line that joins them, in Fig. 5b represent the mixed potential at each pH that separate the anodic and cathodic current responses.)

the construction of TK diagrams for other metals/alloys/minerals in aqueous media containing various ligands or complexing species.

It is important to mention here that the Faradaic efficiency of any chemical process can not be measured directly from these diagrams. For instance, to measure the Faradaic efficiency of Cu dissolution at 0.4 V and pH 2, the overall dissolution rate or current can be estimated from the TK diagram. This current can be applied for a specific period (i.e., 1 h) in a separate experiment and total mass loss of Cu from the Cu-RDE electrode can be measured gravimetrically and may be used to calculate the Faradaic efficiency. This work is not in the scope of this study but may be considered in future. Similarly, it is difficult to decipher any information about the nature of dissolution

(uniform or localized corrosion) from these TK diagrams. Additional electrochemical analysis (i.e. cyclic polarization, galvanostatic or potentiostatic tests) and surface topography examination would become necessary to identify the dissolution mechanism.

Conclusions

We describe a method to develop the TK diagrams for the Cu-H_2O-acetate and Cu-H_2O systems at 25 °C. These diagrams can be used for process development and optimization. The TK diagrams were constructed by using electrochemical test data obtained by LSV scanning of a Cu-RDE under optimized conditions. The LSV scans were obtained at a 0.1667 mV/s scan rate and at 500 rpm to minimize the current contribution associated with the double layer charging and to avoid mass transport limitations, respectively. The Cu-RDE rotation rate was selected based on the physical characterization of the electrolytes and the electrochemical response of the system to varying rotation rates. An approximately 73% decrease in the diffusion layer thickness was observed at a 500 rpm rotation rate. The LSV curves of the Cu-RDE obtained in electrolytes of different pH, ranging from 1 to 13, were plotted as contour maps highlighting the current response on the E_h-pH scale. The LSV scans had negligible uncertainty in the current response, which confirms that the TK diagrams are reproducible. The same method can be applied to construct the TK diagrams for other metals, alloys, and minerals under different conditions.

Declaration of Competing Interest

Author(s) declare that there are no competing financial or non-financial interests associated with this manuscript.

Acknowledgment

The financial support from the Natural Sciences and Engineering Research Council of Canada (NSERC) is highly appreciated.

Supplementary materials

Supplementary material associated with this article can be found, in the online version, at doi:10.1016/j.mex.2021.101539.

References

[1] H.P. Hermansson, Copper Thermodynamics in the Repository Environment up to 130 °C, Swedish Radiation Safety Authority, Stockholm, Sweden, Report No. SSM 2010:09 (2010) 60 https://inis.iaea.org/search/search.aspx?orig_q=RN:42089092.
[2] K. Mairaj Deen, N. Mehrjoo, E. Asselin, Thermo–Kinetic diagrams: the Cu–H_2O–Acetate and the Cu-H_2O systems, J. Electroanal. Chem. (2021) 115467.
[3] S. Roy, H. Zebardast, E. Asselin, On the development of thermo-kinetic Eh-pH diagrams, Metall. Mater. Trans. B 43 (6) (2012) 1277–1283.
[4] E. McCafferty, in: Introduction to Corrosion Science, Springer Science & Business Media, 2010, p. 291.
[5] S. Esmailzadeh, M. Aliofkhazraei, H. Sarlak, Interpretation of cyclic potentiodynamic polarization test results for study of corrosion behavior of metals: a review, Prot. Metals Phys. Chem. Surf. 54 (2018) 976–989.
[6] F. Mansfeld, M. Kendig, Technical note: concerning the choice of scan rate in polarization measurements, Corrosion 37 (9) (1981) 545–546.
[7] J. Zheng, Y. Yan, B. Xu, Correcting the hydrogen diffusion limitation in rotating disk electrode measurements of hydrogen evolution reaction kinetics, J. Electrochem. Soc. 162 (14) (2015) F1470–F1481.
[8] D.G. Leaist, P.A. Lyons, Multicomponent diffusion of electrolytes with incomplete dissociation. Diffusion in a buffer solution, J. Phys. Chem. 85 (12) (1981) 1756–1762.
[9] P.N. Kaloyerou, Basic Concepts of Data and Error Analysis, Springer, 2018.
[10] H.H. Huang, The Eh-pH diagram and its advances, Metals 6 (1) (2016) 23.